NMRlipids IV: Headgroup & glycerol backbone structures, and cation binding in bilayers with PS lipids

Pavel Buslaev,[1] Tiago M. Ferreira,[2] Ivan Gushchin,[1] Matti Javanainen,[3] Batuhan Kav,[4] Jesper J. Madsen,[5] Markus Miettinen,[4] Josef Melcr,[3] Ricky Nencini,[3] O. H. Samuli Ollila,[3, 6, *] and Thomas Piggot **1.Authorlist is not yet complete**[7]

[1]*Moscow Institute of Physics and Technology*
[2]*Halle, Germany*
[3]*Institute of Organic Chemistry and Biochemistry, Academy of Sciences of the Czech Republic, Prague 6, Czech Republic*
[4]*Potsdam, Germany*
[5]*Department of Chemistry, The University of Chicago, Chicago, Illinois 60637, United States of America*
[6]*Institute of Biotechnology, University of Helsinki*
[7]*Southampton, United Kingdom*
(Dated: September 7, 2018)

Phosphatidylserine (PS) is the most common negatively charged lipid in eykaryotic membranes. PS lipids interact with signaling and other proteins via electrostatic interactions and direct binding, and induce membrane fusion and phase separation together with calcium ions. Molecular details of these phenomena are not well understood because accurate models to interpret the experimental data has not been available. Here, we collect a set of experimental NMR data which could be used together with molecular dynamics (MD) simulations to interpret the lipid headgroup structures and details of ion binding in pure and mixed PS and PS:PC lipid bilayers. Aiming to interpret the data, we use the open collaboration method to go through the available MD simulation models for PS lipids. However, none of the models reproduce the experimental data with sufficient accuracy to interpet the structural details of lipid headgroups or ion binding details in lipid bilayers containing PS lipids. In contrast to PC lipids, the tested MD simulation models do not correctly reproduce the qualitative response of PS lipid headgroups to the bound ions or changes in the lipid composition. Our results pave the way for the model improvement to correctly describe negatively charged membranes and their interactions with ions.

INTRODUCTION

Phosphatidylserine (PS) is the most common negatively charged lipid in eykaryotic membranes. PS lipids compose 8.5% of total lipid weight of erythrocytes, but the abundance varies between different organelles up to 25-35% in plasma membrane [1–3]. Despite of the relatively low abundance, PS lipids are important signaling molecules. They interact with signaling proteins [2], regulate surface charge and protein localization [4], and induce protein aggregation [5, 6]. Some domains spesifically interact PS lipids, while others are attracted by general electrostatics and the binding can be regulated by calcium [2]. Therefore, the structural details of lipid headgroups and the details of cation binding are crucial for the PS mediated signaling processes.

Previous experimental studies have concluded that PS headgroups are more rigid than phophocholines (PC) due to the hydrogen bonding network or electrostatic interactions [7, 8]. Multivalent cations and Li$^+$ are able to form strong dehydrated molecular complexes with PS lipids, while monovalent ions interact more weakly with PS containing bilayers [9–19]. The dehydrated complexes of PS headgroup and calcium ions can also lead to the phase separation [9, 10, 14–18]. On the other hand, some studies propose that the specific binding affinity is similar to the negatively charged and zwitterionic lipids and that the increased cation binding to negatively charged lipid bilayer arise only due to the increase of local cation concentration in the vicinity of membranes [20, 21]. Dilution of bilayers with PC lipids makes PS headgroups less rigid and reduces propensity for the formation of strong complexes with multivalent ions [7, 8, 17, 18]. The molecular level interpretation of these observations is, however, not available.

Several classical molecular dynamics (MD) simulation studies are done to understand PS headgroups, their influence on lipid bilayer properties and interactions with ions [19, 22–32]. However, the recent comparisons of PC lipid headgroup and glycerol backbone C-H bond order parameters calculated from different simulation models revealed that improvements in the current force fields are needed to correctly reproduce the headgroup structure and ion binding to lipid bilayers [33–35]. The ion binding affinity to POPC bilayer was then improved by implicitly including the electronic polarizability using the electronic continuum correction [36]. Here, we collect the set of experimentally measured lipid headgroup and glycerol backbone C-H bond order parameters, which can be used to evaluate the quality of headgroup structure and the ion binding affinity in MD simulations of lipid bilayers containing PS lipids. The available MD simulation models of PS are then compared against the collected experimental data. The results pave the way for the development of MD simulation force fields that correctly describe PS lipid headgroup structure and its interactions with ions. Such models are expected to be useful in elucidating the biological role of PS and other lipid headgroups because glycerol backbone and lipid headgroups behave similarly in model membranes and in bacteria [20, 37, 38].

TABLE I: List of MD simulations of pure PS bilayers without additional salt. CKPM refers to the version with Berger/Chiu NH_3 charges compatible with Berger (i.e. the NH_3 group having the same charges as in the $N(CH_3)_3$ group of the PC lipids; 'M' stands for Mukhopadhyay after the first published Berger-based PS simulation that used these charges [24]) and CKP refers to the version with more Gromos compatible version (i.e. the charges for the NH_3 group taken from the lysine side-chain).

lipid/counter-ions	force field for lipids / ions	$^a N_l$	$^b N_w$	$^c N_c$	$^d T$ (K)	$^e t_{sim}$(ns)	$^f t_{anal}$ (ns)	^{g}files
DOPS/Na^+	CHARMM36 [29]	128	4480	0	303	500	100	[39]
DOPS/Na^+	CHARMM36ua [?] 2.	128	4480	0	303	500	100	[40]
DOPS/Na^+	Slipids [41]	128	4480	0	303	500	100	[42]
DOPS/Na^+	Slipids [41]	288	11232	0	303	200	100	[43]
DOPS/Na^+	Berger [24]	128	4480	0	303	500	100	[44]
DOPS/Na^+	GROMOS-CKPM [?] 3.	128	4480	0	303	500	100	[45]
DOPS/Na^+	GROMOS-CKP [?] 4.	128	4480	0	303	500	100	[46]
DOPS/Na^+	lipid17 [47] / JC [48]	128	4480	0	303	600	100	[49]
DOPS/Na^+	lipid17 [47] / ff99 [50]	128	4480	0	303	600	100	[51]
POPS/Na^+	CHARMM36 [29]	128	4480	0	298	500	100	[52]
POPS/K^+	CHARMM36 [29]	128	4480	0	298	500	100	[53]
POPS/Na^+	CHARMM36ua [?] 5.	128	4480	0	298	500	100	[54]
POPS/Na^+	Slipids [41]	128	4480	0	298	500	100	[55]
POPS/Na^+	Berger [?]	128	4480	0	298	500	100	[56]
POPS/Na^+	MacRog [57]	128	4480	0	298	500	100	[58]
OPPS/Na^+	MacRog [57]	128	5120	0	298	200	100	[59]
POPS/Na^+	GROMOS-CKPM [?] 6.	128	4480	0	298	500	100	[60]
POPS/Na^+	GROMOS-CKP [?] 7.	128	4480	0	298	500	100	[61]
POPS/Na^+	lipid17 [47] / JC [48]	128	4480	0	298	600	100	[62]
POPS/Na^+	lipid17 [47] / ff99 [50]	128	4480	0	298	600	100	[63]

^{a}Number of lipid molecules with largest mole fraction
^{b}Number of water molecules
^{c}Number of additional cations
^{d}Simulation temperature
^{e}Total simulation time
^{f}Time used for analysis
^{g}Reference for simulation files

METHODS

Solid state NMR experiments

Headgroup and glycerol backbone C-H bond order parameters of POPS were determined from chemical-shift resolved dipolar splittings measured with a R-type Proton Detected Local Field (R-PDFL) experiment [82] and corresponding order parameter signs were measured with a S-DROSS experiment [83] using natural abundance ^{13}C solid state NMR spectroscopy as described previously [84, 85]. The experiments were done in a Bruker Avance III 400 spectrometer operating at a ^{1}H Larmor frequency of 400.03 MHz. Magic angle spinning (MAS) of the sample was used at a frequency of 5.15 kHz (R-PDLF experiment) and 5 kHz (S-DROSS experiment). The following experimental setups were used.

R-PDLF experiment. The parameters are described according to Figures 1c and 2c of the original reference for the R-PDLF experiment [82]. The refocused-INEPT delays τ_1 and τ_2 were 1.94 ms and 0.97 ms, respectively. Radio fre-

quency pulses with the nutation frequencies: 46.35 kHz ($R18_1^7$ pulses), 63.45 kHz (^{13}C 90° and 180°), 50 kHz (SPINAL64 ^{1}H decoupling pulses). The t_1 increment was equal to 10.79 μs $\times 18 \times 2$ and 32 points in the indirect dimension were recorded using 1024 scans for each, with recycle delay of 5 s and a spectral with of 149.5 ppm.

S-DROSS experiment. The parameters are described according to Figures 1b and 1c of the original reference for the S-DROSS experiment [83]. The refocused-INEPT delay δ_2 was 1.19 ms. The τ_1 and τ_2 in the S-DROSS recoupling blocks R were set as 39.4 μs and 89.4 μs, respectively. Radio frequency pulses with the nutation frequencies: 63.45 kHz (^{13}C 90° and 180°), 50 kHz (^{1}H SPINAL64 decoupling). The t_1 increment (dipolar recoupling dimension) was 800 μs and a total of 8 points along t_1 were measured using 1024 scans for each with a recycle delay of 5 s and a spectral with of 149.5 ppm.

NMR numerical simulations The numerical simulations of S-DROSS curves were performed with the SIMPSON simulation package using the ^{13}C–^{1}H dipolar couplings deter-

TABLE II: List of POPC:POPS mixture simulations with different amounts of added ions. The salt concentrations calculated as [salt]=$N_c \times$[water]$/N_w$, where [water] = 55.5 M. these correspond the concentrations reported in the experiments by Roux et al. [17].

lipid/counter-ions	force field for lipids / ions	$^a C_{ci}$ (M)	[CaCl$_2$] (M)	$^b N_l$	$^c N_w$	$^d N_c$	^{e}T (K)	$^f t_{sim}$(ns)	$^g t_{anal}$ (ns)	^{h}files
POPC:POPS (5:1)/K$^+$	CHARMM36 [29, 64]	0	0	110:22	4935	0	298	100	100 **8.**	[65]
POPC:POPS (5:1)/K$^+$	CHARMM36 [29, 64]	0	0	250:50	?	0	298	200	?	[?] **9.**
POPC:POPS (5:1)/K$^+$	CHARMM36 [29, 64]	0	0	110:22	4620	0	298	500	100	[66]
POPC:POPS (5:1)/Na$^+$	CHARMM36 [29, 64]	0	0	110:22	4620	0	298	500	100	[67]
POPC:POPS (1:1)/K$^+$	CHARMM36 [29, 64]	0	0	150:150	?	0	298	200	?	[?] **10.**
POPC:POPS (5:1)	CHARMM36 [29, 64, 68]	0	0.15 **11.**	250:50	?	?	298	200	?	[?] **12.**
POPC:POPS (5:1)	CHARMM36 [29, 64, 68]	0	1 **13.**	250:50	?	?	298	200	?	[?] **14.**
POPC:POPS (5:1)/K$^+$	MacRog [57]	0	0	120:24	5760	0	298	400	250	[69]
POPC:POPS (5:1)/K$^+$	MacRog [57]	0	0.10	120:24	5760	10	298	600	300	[69]
POPC:POPS (5:1)/K$^+$	MacRog [57]	0	0.30	120:24	5760	31	298	600	300	[69]
POPC:POPS (5:1)/K$^+$	MacRog [57]	0	1.00	120:24	5760	104	298	600	300	[69]
POPC:POPS (5:1)/K$^+$	MacRog [57]	0	3.00	120:24	5760	311	298	600	300	[69]
POPC:POPS (5:1)/K$^+$	MacRog [57]	0.50	0	120:24	5760	52	298	300	200	[70]
POPC:POPS (5:1)/K$^+$	MacRog [57]	1.00	0	120:24	5760	104	298	300	200	[70]
POPC:POPS (5:1)/K$^+$	MacRog [57]	2.00	0	120:24	5760	208	298	300	200	[70]
POPC:POPS (5:1)/K$^+$	MacRog [57]	3.00	0	120:24	5760	311	298	300	200	[70]
POPC:POPS (5:1)/K$^+$	Lipid14/17 [47, 71]	0	0	120:24	5760	0	298	500	200	[72]
POPC:POPS (5:1)/K$^+$	Lipid14/17 [47, 71]	0.5**15.**	0	120:24	5760	?	298	300	200	[73]
POPC:POPS (5:1)/K$^+$	Lipid14/17 [47, 71]	1**16.**	0	120:24	5760	?	298	300	200	[73]
POPC:POPS (5:1)/K$^+$	Lipid14/17 [47, 71]	2**17.**	0	120:24	5760	?	298	300	200	[73]
POPC:POPS (5:1)/K$^+$	Lipid14/17 [47, 71]	3**18.**	0	120:24	5760	?	298	300	200	[73]
POPC:POPS (5:1)/K$^+$	Lipid14/17 [47, 71]	4**19.**	0	120:24	5760	?	298	300	200	[73]
POPC:POPS (5:1)/Na$^+$	Lipid14/17 [47, 71]	0	0	120:24	5760	0	298	500	200	[74]
POPC:POPS (5:1)/Na$^+$	Lipid14/17 [47, 71]	0.5**20.**	0	120:24	5760	?	298	300	200	[75]
POPC:POPS (5:1)/Na$^+$	Lipid14/17 [47, 71]	1**21.**	0	120:24	5760	?	298	300	200	[75]
POPC:POPS (5:1)/Na$^+$	Lipid14/17 [47, 71]	2**22.**	0	120:24	5760	?	298	300	200	[75]
POPC:POPS (5:1)/Na$^+$	Lipid14/17 [47, 71]	3**23.**	0	120:24	5760	?	298	300	200	[75]
POPC:POPS (5:1)/Na$^+$	Lipid14/17 [47, 71]	4**24.**	0	120:24	5760	?	298	300	200	[75]
POPC:POPS (5:1)/Na$^+$	Lipid14/17 [47, 71]	0	0	60:12	?	0	298	?	?	[?] **25.**
POPC:POPS (5:1)/Na$^+$	Lipid14/17 [47, 71]	0**26.**	0.03	60:12	?	?	298	?	?	[?] **27.**
POPC:POPS (5:1)/Na$^+$	Lipid14/17 [47, 71]	0**28.**	0.17	60:12	?	?	298	?	?	[?] **29.**
POPC:POPS (5:1)/Na$^+$	Lipid14/17 [47, 71]	0**30.**	0.36	60:12	?	?	298	?	?	[?] **31.**
POPC:POPS (4:1)/Na$^+$	Berger [24, 76]	0	0	102:26	4290	0	310	?	?	[?] **32.**
POPC:POPS (4:1)/Na$^+$	Berger [24, 76]**33.**	1.03	0	102:26	4290	80	310	200	50	[77]
POPC:POPS (4:1)	Berger [24, 76]	0	0.12^i	104:24	4306	24	310	300	100	[78]
POPC:POPS (4:1)	Berger [24, 76]	0	0.715^j	104:24	4306	72	310	300	100	[79]
POPC:POPS (5:1)/Na$^+$	GROMOS-CKP [?]	0	0	110:22	?	0	298	500	100	[80]
POPC:POPS (5:1)/Na$^+$	GROMOS-CKPM [?]	0	0	110:22	?	0	298	500	100	[81]

^{a}Excess Na$^+$ or K$^+$ concentration
^{b}Number of lipid molecules with largest mole fraction
^{c}Number of water molecules
^{d}Number of additional cations
^{e}Simulation temperature
^{f}Total simulation time
^{g}Time used for analysis
^{h}Reference for simulation files
^{i}Calculation of concetration complicated due the scaled ions. Concentration taken as reported in the delivered data.
^{j}Calculation of concetration complicated due the scaled ions. Concentration taken as reported in the delivered data.

mined by the R-PDLF experiments or calculated from known ^{2}H quadrupolar couplings as input. Chemical shift anisotropy and homonuclear couplings were neglected, and the input file *rep2000* was used to simulate the random distribution of bilayer orientations in the samples studied.

Sample preparation **34.Sample preparation should be described.**

Molecular dynamics simulations

Molecular dynamics simulation data was collected using the Open Collaboration method [33]. The NMR-lipids project blog (`nmrlipids.blogspot.fi`) and the GitHub repository (`github.com/NMRLipids/NMRlipidsIVotherHGs`) were used as the communication platforms. The simulated systems are listed in Tables I (pure PS systems without additional ions) and II (mixed PC:PS systems with various ions concentrations). Simulation details are given in the SI. The simulation data is also indexed in the searchable database (`nmrlipids.fi`), and in the NMRlipids/MATCH GitHub repository (`https://github.com/NMRLipids/MATCH`).

The C-H bond order parameters were calculated directly from the definition

$$S_{CH} = \frac{1}{2} \langle 3\cos^2\theta - 1 \rangle, \tag{1}$$

where θ is the angle between the C-H bond and the membrane normal. Angular brackets point to the average over all sampled configurations. **35.Error estimation should be discussed.** The number density profiles were calculated using *gmx density* tool from Gromacs sofware package [86].

Comparison of ion binding to negatively charged lipid bilayers between simulations and experiments using the electrometer concept

The order parameters of α and β carbons in PC lipids can be used to measure the ion binding affinity because they decrease proportionally to the amound of bound positive charge to a bilayer [87–89]. This molecular electrometer concept is especially useful for the comparison between simulations and experiments because the headgroup order parameters can be directly calculated from simulations [34]. Also the headgroup order parameters of negatively charged PS and PG lipids exhibit systemic, but less characterized dependence on the bound charge [17, 90–92]. Therefore, the ion binding affinity to negatively charged bilayers can be better characterized by measuring the PC headgroup order parameters from mixed bilayers [17, 18, 92], see section S2 in the supplementary information.

Before using the PC headgroup order parameters to quantify the ion binding affinity, it is important to quantify their response to the known amount of bound charge [34, 36]. This

can be done using the experimental data from the mixtures of monovalent cationic surfactants (dihexadecyldimethylammonium) and POPC [36, 93], see section S3 in the supplementary information. In this work, we also quantify the response of PC headgroup order parameters to the negatively charged PS headgroups, which also follows the electrometer concept in the experiments [38], see section S2 in the supplementary information.

In the experiment from the literature used in this work [7, 17], the lipids were first soluted to the buffer and then centrifuged to a pellet which was used in the measurements. In such experiments the samples contain approximately 10 wt % of lipids [7, 17, 94], which is less than in gravimetric experiments (60 wt %) and simulations (approx. 50-60 wt %) in this work. Since multilamellar structures of pure PS lipids swell due to the electrostatic repulsion, the larger repeat distances are expected in samples with lower lipid concentrations [95]. However, the PS headgroup order parameters from gravimetric sample are in good agreement with centrifuged sample (Fig. 2) and the equilibrium repeat distance decreases already above 500 mM concentration of monovalent ions close to the simulation box sizes [95, 96]. Therefore, the hydration levels of multilamellae are expected to be sufficiently similar in simulations and the reference experiments.

Two different definitions for the salt concentrations have been used when electrometer concept is applied to study ion binding affinity. The concentrations are reported either in water before solvating the lipids [17, 34, 87] or in bulk water after solvating the lipids [36, 88]. In this work, we use the former definition to be consistent with the reference experimental data [17]. The used definition has only a marginal effect to the results is simulations with realistic ion binding affinity.

RESULTS AND DISCUSSION

Headgroup and glycerol backbone order parameters of POPS from ^{13}C NMR

36.How is the peak assignment done?
The INEPT and 2D R-PDLF experiments from POPS sample give well resolved spectras for all the carbons in headgroup and glycerol backbone region, except for g_3 for which the resolution was not sufficient to determine the numerical value of the order paramater (Fig. 1). Slices of the R-PDFL spectra (Fig. 1 C)) show a single splitting for the β-carbon with the order parameter value of 0.12, and a superposition of a large and a very small splitting for the α-carbon. The larger splitting gives a order parameter value of 0.09, while the numerical value from the small splitting cannot resolved with the available resolution. Since the R-PDFL and previous ^{2}H NMR experiments [7, 18] give only the absolute values of order parameters, we determined the signs of PS headgroup and glycerol backbone order parameters using the S-DROSS experiment [83]. The S-DROSS slice for the β-carbon (Fig. 1 D)) clearly shows that the order parameter is negative, which

FIG. 1: The headgroup and glycerol backbone region of the (A) INEPT spectrum and (B) 2D R-PDLF spectra. (C) Experimental SDROSS data (points) and SIMPSON simulations (blue lines) with the order parameter values of -0.12 for the β-carbon, and 0.09 and -0.02 for the α-carbon slittings. The S-DROSS curve from SIMPSON simulation with positive value for the smaller α-carbon order parameter (dashed grey).

FIG. 2: Headgroup and glycerol backbone order parameters of POPS measured in this work compared with the values from DOPS (^{2}H NMR, 0.1M of NaCl) [7] and POPC (^{13}C NMR) [84] experiments. Signs of the PS order parameters are measured in this work. Signs of the PC order parameters are measured in Ref. [85].

is confirmed by SIMPSON simulations. The beginning of the S-DROSS slice suggests that the higher order parameter of the α-carbon is positive and the deviation towards negative values with the longer T_1 times suggests that the smaller order parameter is negative. This is confirmed by a SIMPSON simulation where the value of -0.02 was taken from ^{2}H NMR experiment [18] for the smaller order parameter. The literature value was used because the resolution of our experiment was not sufficient to determine the small value of the order parameter. The S-DROSS curve from SIMPSON simulation with a positive value for the smaller order parameter (dashed grey in Fig. 1 D)) did not agree with the experiment, confirming the interpretation that the smaller order parameter is negative.

The headgroup and glycerol backbone order parameters of POPS measured in this work are in good agreement with the previously reported values from ^{2}H NMR experiments of DOPS [7] (Fig. 2). When compared with the previously measured values for POPC [84] (Fig. 2), the β-carbon order parameter is significantly more negative and α-carbon experiences a significant forking in PS headgroup. These features have been intepreted to arise from a rigid PS headgroup con-

formation, stabilized by hydrogen bonds or electrostatic interactions [7, 8], but detailed structrural interpretation is not available.

Headgroup and glycerol backbone in simulations of PS lipid bilayers without additional ions

The headgroup and glycerol backbone of PS lipids show wide variety between different simulation models in the order parameters and structures (Figs. 3 and 4), as previously observed also for PC lipids. The models for PS lipids perform generally less well than for PC lipids in the previous study (Figs. 2 and 4 in Ref. [33] vs. Figs. 3 and 5). Therefore, interpretation of structural differences between PC and PS headgroups from simulations is not straightforward.

The best performing models, Slipids, CHARMM36 and CHARMM36ua, reproduce the larger forking of the α-carbon and the Slipids model reproduces also the lower of the β-carbon order parameter when comparing the PS results to PC (Fig. 2 in Ref. 33 vs. Fig. 3). Interestingly, the headgroup structures of these models share significant similarities and are distinct from other models (Figs. 4 and S6). The distribution of the dihedral angle for C_α-C_β-C_γ-O_γ shows a sin-
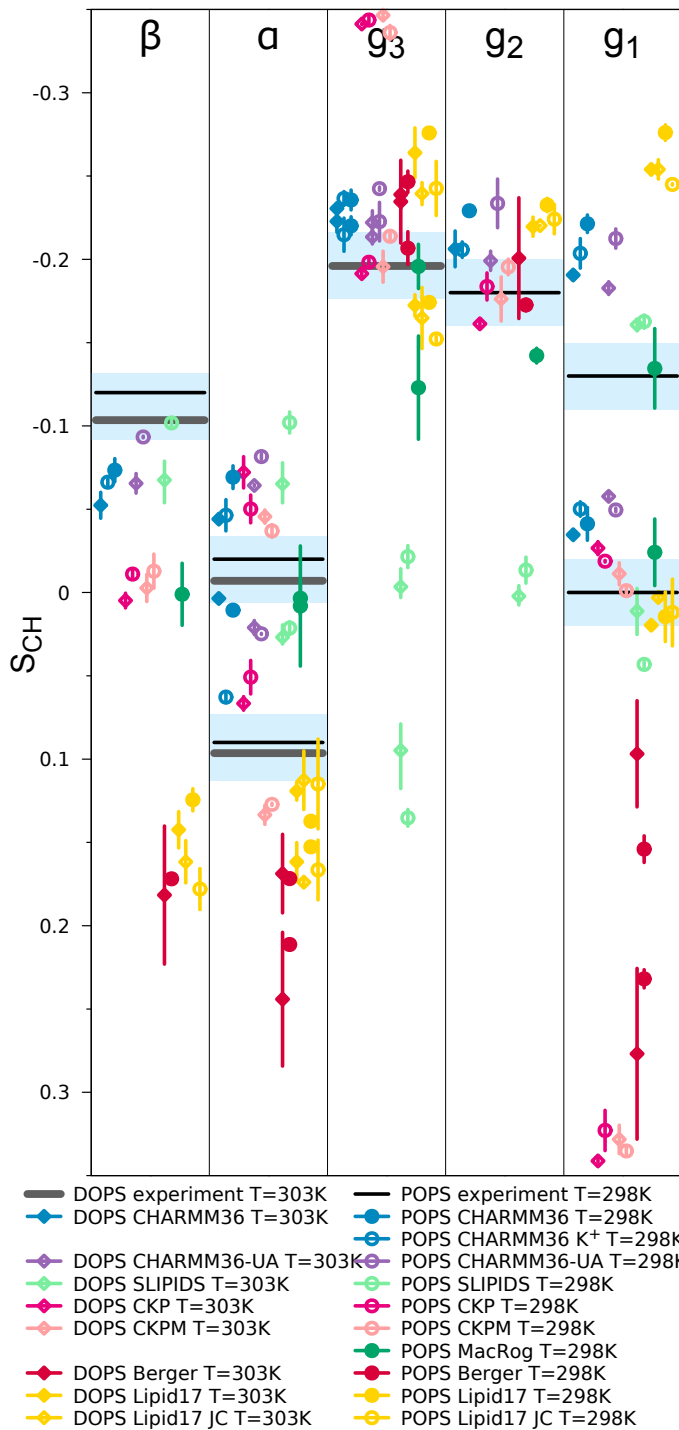
FIG. 3: Order parameters for PS headgroup and glycerol backbone from simulations with different models and experiments without CaCl$_2$. All DOPS data at 303 K, POPS at 298 K. Experimental data from [7] contain 0.1 M of NaCl. Signs are taken from experiments for POPS described in Supplementary Information. The vertical bars shown are not error bars, but demonstrate that we had at least two data sets; the ends of the bars mark the extreme values from the sets, and the dot marks their measurement-time-weighted average.

gle narrow maximum close to 120° in the best three models, while other models give several maxima in different locations (Fig. S6). The restricted motion is also visible in the sampled conformations (Fig. 4) and might manifest the increased rigidity anticipated from the early experimental studies [7, 8]. Another distinct feature in the three best performing models is the distribution of N-C$_\beta$-C$_\alpha$-O$_\alpha$ dihedral, which gives a large maxima close to 300° and a smaller maxima close to 60°. This is also visible in the sampled structures (Fig. 4). **39.There seems to be discrepancy between structures and dihedral distributions for CHARMM36ua.** The glycerol backbone order parameters of C$_2$ and C$_3$ from Slipids simulations differ significantly from the other simulation results and experiments (Fig. 3), as observed previously also for PC lipids [33]. The origin of this difference is more difficult to track without more elaborate analysis, because different models show very complicated patterns of distinct structures in the glycerol backbone region (Figs. 4 and S6).

40.POPS/OPPS issue with MacRog model is in progress: https://github.com/NMRLipids/NMRlipidsIVotherHGs/issues/16

Counterion binding to lipid bilayers containing PS lipids

Membranes containing PS lipids are always accomppanied with counterions, which modulate electrostatic interactions between lipids and other biomolecules. Counterions are also suggested screen the repulsion between charged lipid headgroups in MD simulations and reduce the area per lipid of PS bilayers to be smaller than in PC bilayers [23–25]. The counterion density profiles along membrane normal show significant differences between simulation models (Fig. 6). The strongest counterion binding, i.e., the lowest concentrations in bulk water, are observed in MacRog, Berger and Lipid17/JC simulations. CHARMM36, CHARMM36ua and Gromos-CKP models exhibit two local maxima in counterion density, while a single maxima is observed in the other models. **41.More detailed discussion may be possible after comparing monovalent ion binding to bilayers between CHARMM simulations and experiments. Also, section S6 should be finished.** Area per lipid is in agreement with experiments [30] only in the Gromos-CKP models, while other models give significantly lower values (Fig. 6). The difference cannot be explained by the electrostatic screening of the headgroup repulsion due to counterion binding because CHARMM36, CHARMM36ua and Slipid models give smaller area per lipid than Gromos-CKP models with similar counterion binding affinity.

To evaluate counterion binding in different simulation models against experimental data [17], we plot the headgroup order parameters measured from POPC:POPS 5:1 mixture as a function of different monovalent ions added to the buffer (Fig. 7). Experimental order parameter data for POPC headgroup in the mixture is available as a function of LiCl and KCl concentrations, while POPS headgroup order parameters are measured also as a function of NaCl. Lithium interacts more strongly with PS headgroups than other monova-
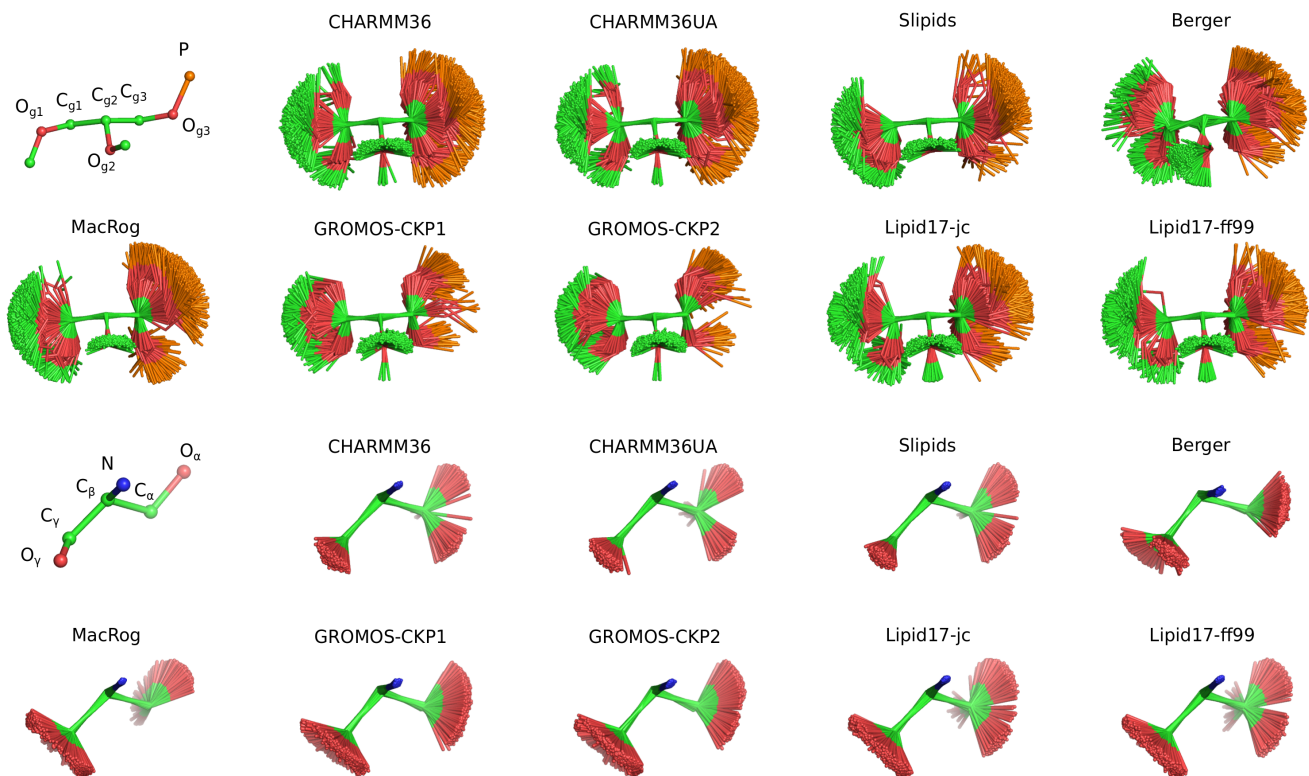
FIG. 4: Overlayed snapshots from glycerol backbone and headgroup region from different simulations of PS lipids.

lent ions [12, 14, 16, 17, 92], as also observed for PC headgroups [97]. This is evident also in the changes of PS headgroup order parameters, which decrease with the addition of lithium but increase with the addition of sodium or potassium (Fig. 7). POPC headgroup order parameters exhibit a clear decrease as a function of LiCl concentration but only modest changes as a function of KCl concentration, indicating significant Li^+ binding but only weak Na^+ binding to the mixture when interpreted using the electrometer concept [87–89]. In simulations with the Berger model, the headgroup order parameter response of POPC to the added NaCl is similar to the experiments of LiCl, indicating overestimated binding affinity of sodium, in line with the results for PC bilayers [34]. Indeed, the sodium density profile shows a significant binding peak in the Berger model (Fig. 8). Potassium binding in the MacRog simulation is significantly weaker (Fig. 8) and the headgroup order parameter changes are also in better agreement with simulations (Fig. 7). **42.Discussion about Lipid17 to be written when we have the density profiles.** All the tested models overestimate the changes of POPS headgroup order parameters as a function of monovalent ions (Fig. 7), suggesting that model development is necessary to interpret the PS headgroup-ion interactions from MD simulations.

Headgroup structure in PS and PC mixtures

Dilution of PS lipid bilayers with PC lipids reduces the propensity of PS headgroup-multivalent ion complexes and is proposed to make PS headgroups less rigid [7, 8, 17, 18]. Therefore, the intermolecular interactions at the headgroup region seems to be important for the physical properties of mixed lipid bilayers. These interactions can be indirectly monitored by measuring the headgroup order parameters from PS:PC mixtures with different molar ratios. The headgroup order parameters of POPC increase in such experiments with increasing amount of POPS (Fig. 9) [38]. This behaviour is generally observed when negatively charged lipids or surfactants are mixed with PC lipids [38, 93] and can be understood by the tilting of lipid headgroup more parallel to the membrane plane according to the electrometer concept [89]. The headgroup order parameters of PS lipids shift closer to zero when bilayer is diluted with PC lipids in experiments (Fig. 9) [7, 17, 38], which is intepreted to indicate reduced rigidity [7, 8].

The increase of POPC headgroup order parameters with the increasing amount of negatively charged POPS lipid is reproduced in MacRog simulations with potassium counterions, but not in Berger simulations with sodium or in CHARMM36 simulations with potassium or sodium conterions (Fig. 9). The observations can be explained using the electrometer concept. The Berger simulation exhibits very strong sodium bind-

8

FIG. 5: Rough subjective ranking of force fields based on Figure 3. Here "M" indicates a magnitude problem, "F" a forking problem; letter size increases with problem severity. Color scheme: "within experimental error" (dark green), "almost within experimental error" (light green), "clear deviation from experiments" (light red), and "major deviation from experiments" (dark red). The Σ-column shows the total deviation of the force field, when individual carbons are given weights of 0 (matches experiment), 1, 2, and 4 (major deviation). For full details of the assessment, see Supplementary Information.

ing (Fig. 8), which surpasses the effect of negatively charged lipids as also the amount of counterions increase with increasing amount of PS. In CHARMM36 simulations, the counterion binding neutralizes the effect of PS and the headgroup order parameters are not changed with increasing amount of PS. Finally, the weak binding of potassium in the MacRog simulations enables the increase of order parameters with the increasing amount of negatively charged PS lipids (Figs. 9 and 8).

Oppositely to experiments, the headgroup order parameter of POPS shift away from zero in CHARM36 simulations when bilayer is diluted with POPC (Fig. 9). In lipid14/17 simulations, the POPS order parameter shift closer to zero when bilayer is diluted with POPC, but the numerical values of order parameters are too far from experiments to enable interpretation of the experimental data. Therefore, we conclude that the force field development is necessary before MD simulations can be used to interpret the interactions between PC and PS headgroups.
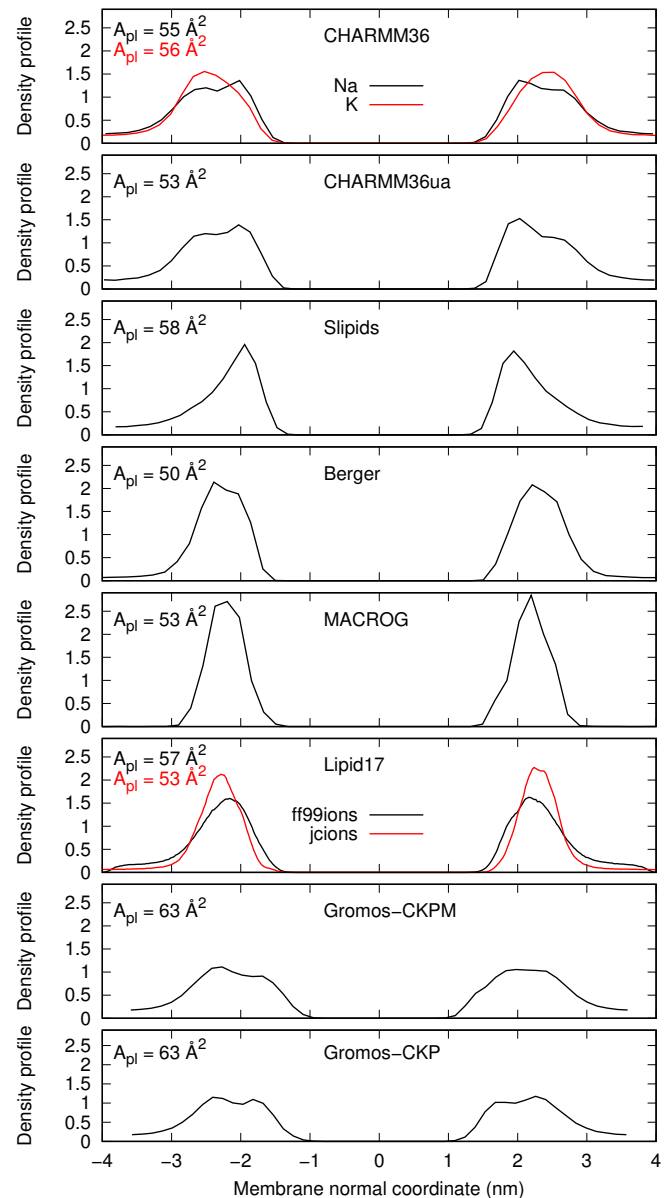
FIG. 6: Counterion densities of POPS lipid bilayer along the membrane normal from simulations with different force fields.

Ca^{2+} binding affinity in bilayers with negatively charged PS lipids

Ion binding affinity to PS containing membranes can be most conveniently measured from PC:PS lipid mixtures where the lipid-ion complexes and phase separation are not observed [15–18]. In addition, the ion binding affinity to such mixtures can be detected using the PC lipid headgroup order parameters, see section S2. As expected from the previous study of pure PC lipid bilayers [34], almost all the tested simulation models overestimate the decrease of POPC headgroup order parameters as a function of Ca^{2+} concentration
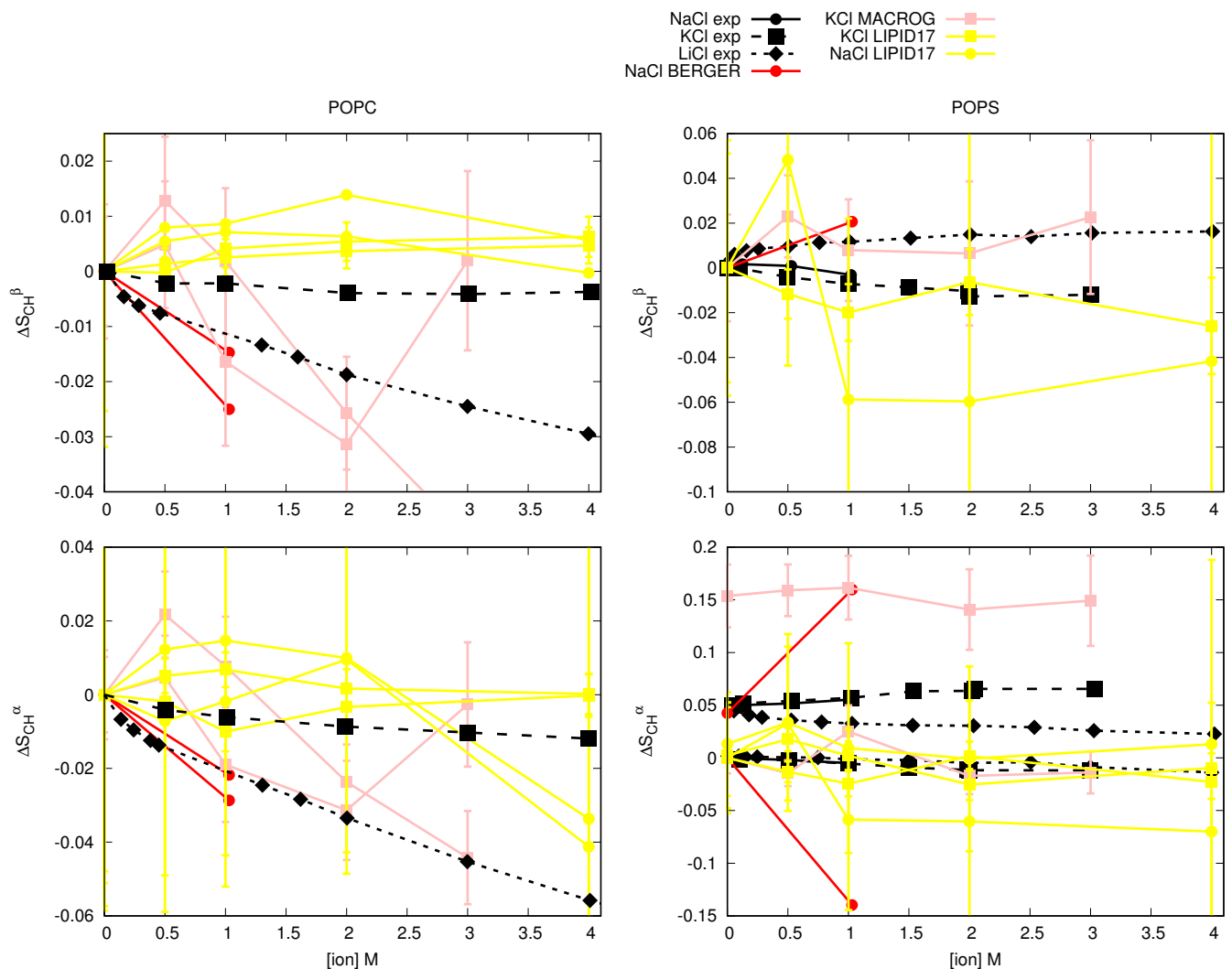
FIG. 7: Changes of the PC (left) and PS (right) headgroup order parameters as a function of added NaCl, KCl and LiCl from POPC:POPS (5:1) mixture at 298 K (except Berger simulations are (4:1) mixture at 310 K). The experimental data is from Ref. 17. The values from counterion-only systems are set as a zero point of y-axis. To correctly illustrate the significant forking of the α-carbon order parameter in PS headgroup (bottom, right), the y-axis is tranferred with the same value for both order parameters such that the lower order parameter value is at zero.

43.CHARMM36 results for this plot would be highly useful.

in POPC:POPS (5:1) mixtures with respect to the experiments [17] (Fig. 10), indicating overestimated calcium binding binding affinity. Only exception is the CHARMM36 model with the NBfix interaction employed for calcium [68], which underestimates the order parameter changes indicating weaker binding affinity than experiments. Notably, CHARMM36 simulations with NBfix corrections [29, 68] give similar binding affinities of calcium and sodium to POPC bilayer (see section **??**), in contrast to the experimental data [87, 88, 97]. Therefore, we conclude that the calcium binding affinity, manifested by the peaks in the density distributions along membrane normal (Fig. 11), is underestimated in CHARMM36 simulations with the NBfix for calcium [68] but overestimated in all the other tested models.

The headgroup order parameters of POPS headgroup measured from POPC:POPS (5:1) mixture exhibit a strong dependence of $CaCl_2$ with small concentrations with a rapid saturation below 100 mM (Fig. 10). The β-carbon order parameter of POPS increase with the added $CaCl_2$ in the experiment and in all the tested simulation models, but simulations significantly overestimated the change. The larger α-carbon order parameter of POPS decrease and the smaller one slightly increase with the added $CaCl_2$ in the experiment. The changes are again significantly overestimated in the simulations, however, in this case all simulations predict qualitatively different behaviour. Notably, the changes of POPS headgroup order parameters are overestimated also in the CHARMM36/NBfix model where the calcium binding affinity was too low. We
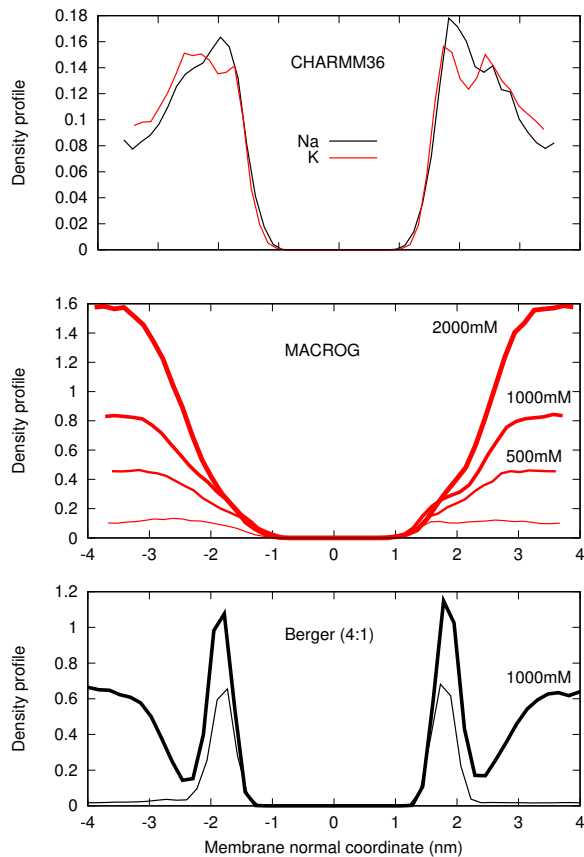
FIG. 8: Counterion density distributions from PC:PS mixtures.

44.Lipid 17 is to be added.

conclude that the effect of bound ions to the headgroup order parameters of POPS is not qualitatively reproduced by the tested simulations models. This is in contrast to previous results for PC headgroup [34], where qualitatively correct reponse to bound ions was observed despite of significant discrepancies in the headgroup structure without additional ions. The response of POPS headgroup order parameters to the bound charge is systematic but less well understood than the responce of PC headgroups used in the electrometer concept [17, 89]. The force field development is necessary to generate MD simulations that could be used to explain the interactions between PS headgroup and calcium ions.

CONCLUSIONS

We have collected a set of experimental NMR order parameter data, which could be combined with MD simulations to interpret the headgroup structure and cation binding details to negatively charged membranes containing PS lipids. Using open collaboration method, we tried to find a MD simu-

lation model which would be sufficiently accurate to interpret the experimental data. However, none of the tested models was accurate enough. In line with the previous study for PC lipids [34], MD simulation models seems to generally overestimate cation binding also to negatively charged bilayers containing PS lipids, with some exceptions. The response of PS lipid headgroup order parameters to the bound cations does not agree with experiments, even in the cases where binding affinity is not overestimated. This is in contrast to the previous results with PC lipids, where the qualitative response of the headgroup order parameters was in agreement with experiments even in the cases where the headgroup structure without ions was not correct and the cation binding affinity was overestimated. In addition, the inaccurate responses of PS headgroup order parameters to the dilution with PC lipids suggests that the PC-PS interactions are not accurately described by the tested models.

Our results pave the way for improving the PS lipid parameters for MD simulations by offering the set of experimental data for the quality measurement, by pinpointing problems areas in the models and suggesting directions for the corrections. Improvements using the electronic continuum correction is already in progress `https://github.com/jmelcr/ecc_lipids`, following the recent work for PC lipids [36].
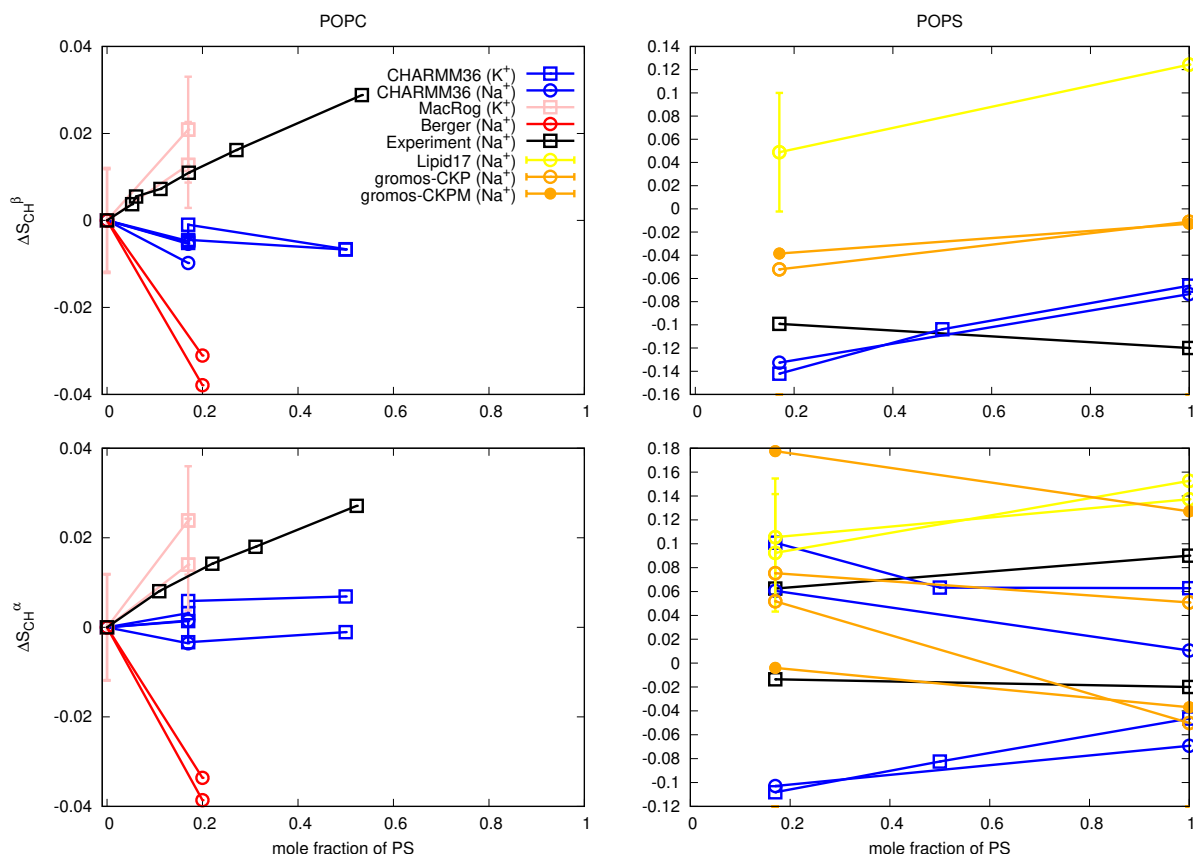
FIG. 9: Changes of PC (left panel) and PS (right panel) headgroup order parameters from POPC:POPS mixtures with increasing amount of POPS. Experimental results of POPC are taken from Ref. 38 (signs are determined as discussed in [33, 35]). Experimental values for POPS in pure bilayer and in mixture are measured in this work and in Ref. 17 at 298K, respectively. Since the experimental data of POPS in pure and diluted mixture come from different experimental sets (13C NMR in this work and 2H NMR from Ref. 17), the experimental change of the order parameter is less accurate than in typical measurements where same technique is used in all conditions, see discussion about qualitative and quantitative accuracy in Ref. 35. For POPC (left panel) the zero point of y-axis is set to the value of pure bilayer. For β-carbon of POPS (right panel, top) the zero point of y-axis is set to the value from POPC:POPS (5:1) mixture. For α-carbon of POPS (right panel, bottom) the y-axis is tranferred with the same value for both order parameters such that the lower order parameter value from POPC:POPS (5:1) mixture is at zero to correctly illustrate the significant forking.

45.Simulation of CHARMM36 at 298K should be maybe rerun with Gromacs 5.

46.Simulation of pure POPC at 298K with Lipid14 would be useful for this plot (only at 303 K is available from NMRlipids I)

47.MacRog simulations of pure POPS with potassium counterions only would be useful for this and other plots.

48.The data from POPC used in Gromos-CKP by would be useful for this plot.

* samuli.ollila@helsinki.fi

[1] M. A. Lemmon, Nat. Rev. Mol. Cell Biol. **9**, 99 (2008).

[2] P. A. Leventis and S. Grinstein, Annual Review of Biophysics **39**, 407 (2010).

[3] L. Li, X. Shi, X. Guo, H. Li, and C. Xu, Trends in Biochemical Sciences **39**, 130 (2014), ISSN 0968-0004.

[4] T. Yeung, G. E. Gilbert, J. Shi, J. Silvius, A. Kapus, and S. Grinstein, Science **319**, 210 (2008).

[5] H. Zhao, E. K. J. Tuominen, and P. K. J. Kinnunen, Biochemistry **43**, 10302 (2004).

[6] G. P. Gorbenko and P. K. Kinnunen, Chemistry and Physics of Lipids **141**, 72 (2006).

[7] J. L. Browning and J. Seelig, Biochemistry **19**, 1262 (1980).

[8] G. Büldt and R. Wohlgemuth, The Journal of Membrane Biology **58**, 81 (1981), ISSN 1432-1424, URL http://dx.doi.org/10.1007/BF01870972.

[9] H. Hauser, E. Finer, and A. Darke, Biochemical and Biophysical Research Communications **76**, 267 (1977), ISSN 0006-291X, URL http://www.sciencedirect.com/science/article/pii/0006291X77907215.

[10] R. J. Kurland, Biochemical and Biophysical Research Communications **88**, 927 (1979), ISSN 0006-291X, URL http://www.sciencedirect.com/science/article/pii/0006291X79914979.

[11] M. Eisenberg, T. Gresalfi, T. Riccio, and S. McLaughlin, Biochemistry **18**, 5213 (1979).

[12] H. Hauser and G. G. Shipley, Biochemistry **22**, 2171 (1983).

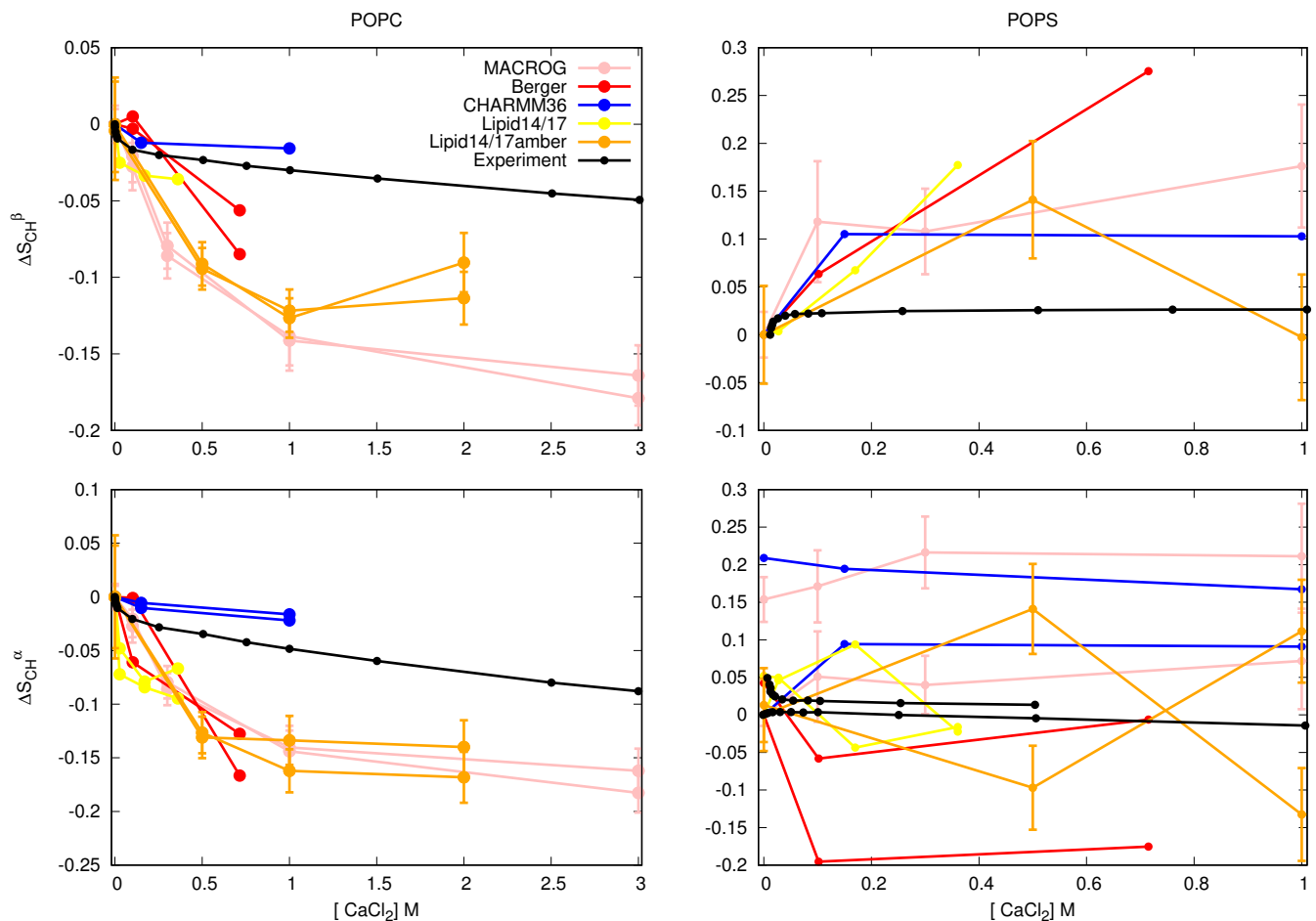[13] R. Dluhy, D. G. Cameron, H. H. Mantsch, and R. Mendelsohn, Biochemistry **22**, 6318 (1983).

FIG. 10: Changes of POPC (left) and POPS (right) headgroup order parameters from POPC:POPS (5:1) mixture as a function CaCl$_2$ concentration from experiments 17 and different simulations at 298K (except the data for Berger model is from simulation of POPC:POPS (4:1) mixture at 310K [32, 98]). The order parameter values from systems without calcium are set as the zero point of y-axis, except for the α-carbon order parameter of POPS (bottom, right) for which the both order parameters are shifted such that the lower order parameter is zero without additional ions to correctly illustrate the forking with different concentrations of calcium. Potassium counterions are used in MacRog simulations and sodium counterions in Lipid14/17 simulations. In CHARMM36 and Berger simulation with added calcium, the charge is neutralized with calcium and monovalent counterions are not present.

49.Upcoming simulations with original CHARMM36 have been mentioned in the blog:
http://nmrlipids.blogspot.com/2017/12/nmrlipids-iv-current-status-and.html?showComment=1520090718976#c5569269391707740056

[14] H. Hauser and G. Shipley, Biochimica et Biophysica Acta (BBA) - Biomembranes 813, 343 (1985), ISSN 0005-2736, URL http://www.sciencedirect.com/science/article/pii/0005273685902512.
[15] G. W. Feigenson, Biochemistry 25, 5819 (1986).
[16] J. Mattai, H. Hauser, R. A. Demel, and G. G. Shipley, Biochemistry 28, 2322 (1989).
[17] M. Roux and M. Bloom, Biochemistry 29, 7077 (1990).
[18] M. Roux and M. Bloom, Biophys. J. 60, 38 (1991).
[19] J. M. Boettcher, R. L. Davis-Harrison, M. C. Clay, A. J. Nieuwkoop, Y. Z. Ohkubo, E. Tajkhorshid, J. H. Morrissey, and C. M. Rienstra, Biochemistry 50, 2264 (2011).
[20] J. Seelig, Cell Biology International Reports 14, 353 (1990), ISSN 0309-1651, URL http://www.sciencedirect.com/science/article/pii/030916519091204H.
[21] C. G. Sinn, M. Antonietti, and R. Dimova, Colloids and Sur-

faces A: Physicochemical and Engineering Aspects 282-283, 410 (2006), a Collection of Papers in Honor of Professor Ivan B. Ivanov (Laboratory of Chemical Physics and Engineering, University of Sofia) Celebrating his Contributions to Colloid and Surface Science on the Occasion of his 70th Birthday.
[22] J. J. López Cascales, J. García de la Torre, S. J. Marrink, and H. J. C. Berendsen, The Journal of Chemical Physics 104, 2713 (1996).
[23] S. A. Pandit and M. L. Berkowitz, Biophysical Journal 82, 1818 (2002).
[24] P. Mukhopadhyay, L. Monticelli, and D. P. Tieleman, Biophysical Journal 86, 1601 (2004).
[25] U. R. Pedersen, C. Leidy, P. Westh, and G. H. Peters, Biochimica et Biophysica Acta (BBA) - Biomembranes 1758, 573 (2006).
[26] P. T. Vernier, M. J. Ziegler, and R. Dimova, Langmuir 25, 1020
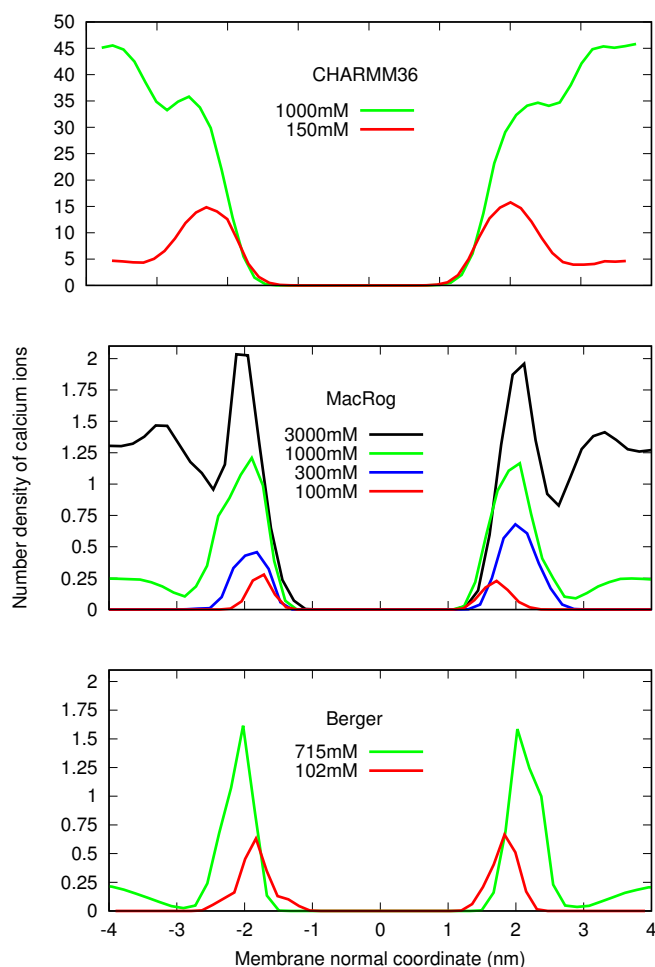
FIG. 11: Ca2+ density profiles from simulations.

50.The CHARMM results are mass densities, number densities should be used when the data by Jesper Madsen is available.

51.Should we include also counterions into the plot?

(2009).

[27] A. Martín-Molina, C. Rodríguez-Beas, and J. Faraudo, Biophysical Journal **102**, 2095 (2012).

[28] P. Jurkiewicz, L. Cwiklik, A. Vojtíšková, P. Jungwirth, and M. Hof, Biochimica et Biophysica Acta (BBA) - Biomembranes **1818**, 609 (2012).

[29] R. M. Venable, Y. Luo, K. Gawrisch, B. Roux, and R. W. Pastor, The Journal of Physical Chemistry B **117**, 10183 (2013).

[30] J. Pan, X. Cheng, L. Monticelli, F. A. Heberle, N. Kucerka, D. P. Tieleman, and J. Katsaras, Soft Matter **10**, 3716 (2014).

[31] S. Vangaveti and A. Travesset, The Journal of Chemical Physics **141**, 245102 (2014).

[32] A. Melcrová, S. Pokorna, S. Pullanchery, M. Kohagen, P. Jurkiewicz, M. Hof, P. Jungwirth, P. S. Cremer, and L. Cwiklik, Sci. Reports **6**, 38035 (2016).

[33] A. Botan, F. Favela-Rosales, P. F. J. Fuchs, M. Javanainen, M. Kanduč, W. Kulig, A. Lamberg, C. Loison, A. Lyubartsev, M. S. Miettinen, et al., J. Phys. Chem. B **119**, 15075 (2015).

[34] A. Catte, M. Girych, M. Javanainen, C. Loison, J. Melcr, M. S. Miettinen, L. Monticelli, J. Maatta, V. S. Oganesyan, O. H. S. Ollila, et al., Phys. Chem. Chem. Phys. **18**, 32560 (2016).

[35] O. S. Ollila and G. Pabst, Biochimica et Biophysica Acta (BBA) - Biomembranes **1858**, 2512 (2016).

[36] J. Melcr, H. Martinez-Seara, R. Nencini, J. Kolafa, P. Jungwirth, and O. H. S. Ollila, The Journal of Physical Chemistry B **122**, 4546 (2018).

[37] H. U. Gally, G. Pluschke, P. Overath, and J. Seelig, Biochemistry **20**, 1826 (1981).

[38] P. Scherer and J. Seelig, EMBO J. **6** (1987).

[39] T. Piggot, *CHARMM36 DOPS simulations (versions 1 and 2) 303 K 1.0 nm LJ switching* (2017), URL https://doi.org/10.5281/zenodo.1129411.

[40] T. Piggot, *CHARMM36-UA DOPS simulations (versions 1 and 2) 303 K 1.0 nm LJ switching* (2017), URL https://doi.org/10.5281/zenodo.1129456.

[41] J. P. M. Jämbeck and A. P. Lyubartsev, Phys. Chem. Chem. Phys. **15**, 4677 (2013).

[42] T. Piggot, *Slipids DOPS simulations (versions 1 and 2) 303 K 1.0 nm cut-off with LJ-PME* (2017), URL https://doi.org/10.5281/zenodo.1129439.

[43] F. Favela-Rosales, *MD simulation trajectory of a fully hydrated DOPS bilayer: SLIPIDS, Gromacs 5.0.4. 2017.* (2017), URL https://doi.org/10.5281/zenodo.495510.

[44] T. Piggot, *Berger DOPS simulations (versions 1 and 2) 303 K 1.0 nm cut-off* (2017), URL https://doi.org/10.5281/zenodo.1129419.

[45] T. Piggot, *GROMOS-CKP DOPS simulations (versions 1 and 2) 303 K with Berger/Chiu NH3 charges and PME* (2017), URL https://doi.org/10.5281/zenodo.1129429.

[46] T. Piggot, *GROMOS-CKP DOPS simulations (versions 1 and 2) 303 K with GROMOS NH3 charges and PME* (2017), URL https://doi.org/10.5281/zenodo.1129447.

[47] I. Gould, A. Skjevik, C. Dickson, B. Madej, and R. Walker, *Lipid17: A comprehensive amber force field for the simulation of zwitterionic and anionic lipids* (2018), in preparation.

[48] I. S. Joung and T. E. Cheatham, The Journal of Physical Chemistry B **112**, 9020 (2008).

[49] B. Kav and M. S. Miettinen, *Molecular dynamics simulation trajectory of an anionic lipid bilayer: 100 mol% DOPS with Na+ counterions using Joung-Cheetham Ions* (2018), B.K acknowledges financial support from International Max Planck Research School on Multiscale Bio-Systems, URL https://doi.org/10.5281/zenodo.1134871.

[50] J. Åqvist, J. Phys. Chem. **94**, 8021 (1990).

[51] B. Kav and M. S. Miettinen, *Molecular dynamics simulation trajectory of an anionic lipid bilayer: 100 mol% DOPS with Na+ counterions using ff99 Ions* (2018), B.K acknowledges financial support from International Max Planck Research School on Multiscale Bio-Systems, URL https://doi.org/10.5281/zenodo.1135142.

[52] T. Piggot, *CHARMM36 POPS simulations (versions 1 and 2) 298 K 1.0 nm LJ switching* (2017), URL https://doi.org/10.5281/zenodo.1129415.

[53] T. Piggot, *CHARMM36 POPS simulations (versions 1 and 2) 298 K 1.0 nm LJ switching with K ions* (2018), URL https://doi.org/10.5281/zenodo.1182654.

[54] T. Piggot, *CHARMM36-UA POPS simulations (versions 1 and 2) 298 K 1.0 nm LJ switching* (2017), URL https://doi.org/10.5281/zenodo.1129458.

[55] T. Piggot, *Slipids POPS simulations (versions 1 and 2) 298 K 1.0 nm cut-off with LJ-PME* (2017), URL https://doi.org/10.5281/zenodo.1129441.

[56] T. Piggot, *Berger POPS simulations (versions 1 and 2) 298 K 1.0 nm cut-off* (2017), URL https://doi.org/10.5281/zenodo.1129425.

[57] A. Maciejewski, M. Pasenkiewicz-Gierula, O. Cramariuc, I. Vattulainen, and T. Róg, J. Phys. Chem. B **118**, 4571 (2014).

[58] T. Piggot, *MacRog POPS simulations (versions 1 and 2) 298 K with corrected PO not OP tails* (2018), URL https://doi.org/10.5281/zenodo.1283335.

[59] M. Javanainen, *Simulation of a pops bilayer* (2017), URL https://doi.org/10.5281/zenodo.1120287.

[60] T. Piggot, *GROMOS-CKP POPS simulations (versions 1 and 2) 298 K with Berger/Chiu NH3 charges and PME* (2017), URL https://doi.org/10.5281/zenodo.1129431.

[61] T. Piggot, *GROMOS-CKP POPS simulations (versions 1 and 2) 298 K with GROMOS NH3 charges and PME* (2017), URL https://doi.org/10.5281/zenodo.1129435.

[62] M. S. Miettinen and B. Kav, *Molecular dynamics simulation trajectory of an anionic lipid bilayer: 100 mol% POPS with Na+ counterions using Joung-Cheatham Ions* (2018), B.K. acknowledges financial support from International Max Planck Research School on Multiscale Bio-Systems., URL https://doi.org/10.5281/zenodo.1148495.

[63] M. S. Miettinen and B. Kav, *Molecular dynamics simulation trajectory of an anionic lipid bilayer: 100 mol% POPS with Na+ counterions using ff99 ions* (2018), B.K. acknowledges financial support from International Max Planck Research School on Multiscale Bio-Systems, URL https://doi.org/10.5281/zenodo.1134869.

[64] J. B. Klauda, R. M. Venable, J. A. Freites, J. W. O'Connor, D. J. Tobias, C. Mondragon-Ramirez, I. Vorobyov, A. D. MacKerell Jr, and R. W. Pastor, J. Phys. Chem. B **114**, 7830 (2010).

[65] O. H. S. Ollila, *POPS+83%popc lipid bilayer simulation at T298K ran CHARMM_GUI force field and Gromacs* (2017), URL https://doi.org/10.5281/zenodo.1011104.

[66] T. Piggot, *CHARMM36 POPS/POPC simulations (versions 1 and 2) 298 K 1.0 nm LJ switching with K ions* (2018), URL https://doi.org/10.5281/zenodo.1182658.

[67] T. Piggot, *CHARMM36 POPS/POPC simulations (versions 1 and 2) 298 K 1.0 nm LJ switching with Na ions* (2018), URL https://doi.org/10.5281/zenodo.1182665.

[68] S. Kim, D. Patel, S. Park, J. Slusky, J. Klauda, G. Widmalm, and W. Im, Biophysical Journal **111**, 1750 (2016), ISSN 0006-3495, URL http://www.sciencedirect.com/science/article/pii/S0006349516307615.

[69] M. Javanainen, *Simulations of popc/pops membranes with cacl_2.* (2017), URL https://doi.org/10.5281/zenodo.1409551.

[70] M. Javanainen, *Simulations of popc/pops membranes with kcl* (2018), URL https://doi.org/10.5281/zenodo.1404040.

[71] C. J. Dickson, B. D. Madej, A. A. Skjevik, R. M. Betz, K. Teigen, I. R. Gould, and R. C. Walker, J. Chem. Theory Comput. **10**, 865 (2014).

[72] B. Kav and M. S. Miettinen, *Amber Lipid17 Simulations of POPC/POPS Membranes with KCl Counterions* (2018), B.K acknowledges financial support from International Max Planck Research School on Multiscale Bio-Systems, URL https://doi.org/10.5281/zenodo.1250969.

[73] B. Kav and M. S. Miettinen, *Amber Lipid17 Simulations of POPC/POPS Membranes with KCl* (2018), B.K acknowledges financial support from International Max Planck Research School on Multiscale Bio-Systems, URL https://doi.org/10.5281/zenodo.1227257.

[74] B. Kav and M. S. Miettinen, *Amber Lipid17 Simulations of POPC/POPS Membranes with NaCl Counterions* (2018), B.K acknowledges financial support from International Max Planck Research School on Multiscale Bio-Systems, URL https://doi.org/10.5281/zenodo.1250975.

[75] B. Kav and M. S. Miettinen, *Amber Lipid17 Simulations of POPC/POPS Membranes with NaCl* (2018), B.K acknowledges financial support from International Max Planck Research School on Multiscale Bio-Systems, URL https://doi.org/10.5281/zenodo.1227272.

[76] D. P. Tieleman, H. J. Berendsen, and M. S. Sansom, Biophys. J. **76**, 1757 (1999).

[77] L. Cwiklik, *MD simulation trajectory of a POPC/POPS (4:1) bilayer with 1M NaCl, Berger force field for lipids and ffgmx for ions* (2017), URL https://doi.org/10.5281/zenodo.838219.

[78] C. Lukasz, *MD simulation trajectory of a POPC/POPS (4:1) bilayer with 102mM CaCl2, Berger force field for lipids, scaled charges for Ca2+ and Cl-* (2017), URL https://doi.org/10.5281/zenodo.887398.

[79] C. Lukasz, *MD simulation trajectory of a POPC/POPS (4:1) bilayer with 715mM CaCl2, Berger force field for lipids, scaled charges for Ca2+ and Cl-* (2017), URL https://doi.org/10.5281/zenodo.887400.

[80] T. Piggot, *GROMOS-CKP POPS/POPC simulations (versions 1 and 2) 298 K with GROMOS NH3 charges and PME* (2018), URL https://doi.org/10.5281/zenodo.1283333.

[81] T. Piggot, *GROMOS-CKP POPS/POPC simulations (versions 1 and 2) 298 K with Berger/Chiu NH3 charges and PME* (2018), URL https://doi.org/10.5281/zenodo.1283331.

[82] S. V. Dvinskikh, H. Zimmermann, A. Maliniak, and D. Sandstrom, J. Magn. Reson. **168**, 194 (2004).

[83] J. D. Gross, D. E. Warschawski, and R. G. Griffin, J. Am. Chem. Soc. **119**, 796 (1997).

[84] T. M. Ferreira, F. Coreta-Gomes, O. H. S. Ollila, M. J. Moreno, W. L. C. Vaz, and D. Topgaard, Phys. Chem. Chem. Phys. **15**, 1976 (2013).

[85] T. M. Ferreira, R. Sood, R. Bärenwald, G. Carlström, D. Topgaard, K. Saalwächter, P. K. J. Kinnunen, and O. H. S. Ollila, Langmuir **32**, 6524 (2016).

[86] M. Abraham, D. van der Spoel, E. Lindahl, B. Hess, and the GROMACS development team, *GROMACS user manual version 5.0.7* (2015), URL www.gromacs.org.

[87] H. Akutsu and J. Seelig, Biochemistry **20**, 7366 (1981).

[88] C. Altenbach and J. Seelig, Biochemistry **23**, 3913 (1984).

[89] J. Seelig, P. M. MacDonald, and P. G. Scherer, Biochemistry **26**, 7535 (1987).

[90] F. Borle and J. Seelig, Chemistry and Physics of Lipids **36**, 263 (1985).

[91] P. M. Macdonald and J. Seelig, Biochemistry **26**, 1231 (1987).

[92] M. Roux and J.-M. Neumann, FEBS Letters **199**, 33 (1986).

[93] P. G. Scherer and J. Seelig, Biochemistry **28**, 7720 (1989).

[94] M. Roux, J.-M. Neumann, M. Bloom, and P. F. Devaux, European Biophysics Journal **16**, 267 (1988).

[95] M. Loosley-Millman, R. Rand, and V. Parsegian, Biophysical Journal **40**, 221 (1982).

[96] R. Rand and V. Parsegian, Biochimica et Biophysica Acta (BBA) - Reviews on Biomembranes **988**, 351 (1989).

[97] G. Cevc, Biochim. Biophys. Acta - Rev. Biomemb. **1031**, 311 (1990).

[98] S. Ollila, M. T. Hyvönen, and I. Vattulainen, J. Phys. Chem. B **111**, 3139 (2007).

ToDo